A methodology for the customized design of colonic stents based on a parametric model

S. Puértolas[a], D. Navallas[a], A. Herrera[b], E. López[c], J. Millastre[d], E. Ibarz[a], S. Gabarre[a], J.A. Puértolas[e], L. Gracia[a*]

[a] Department of Mechanical Engineering, University of Zaragoza, María de Luna 3, 50018 Zaragoza, Spain
[b] Department of Surgery, University of Zaragoza, Domingo Miral s/n, 50009 Zaragoza, Spain
[c] Department of Manufacturing Engineering, University of Zaragoza, María de Luna 3, 50018 Zaragoza, Spain
[d] Department of Gastroenterology, Lozano Blesa University Hospital. Zaragoza, Spain
[e] Department of Material Science, Univ. of Zaragoza, María de Luna 3, 50018 Zaragoza, Spain

*Corresponding author.
E-mail addresses: lugravi@unizar.es

Abstract

The choice of necessary stent properties depends mainly on the length of the stenosis and degree of occlusion. So a stent design with variable radial stiffness along its longitudinal axis would be a good option. The design proposed corresponds to a tube-based stent with closed diamond-shaped cells made from a NiTi alloy. By acting independently on different geometric factors, variable geometries can be obtained with different radial force reactions. A design adjustment according to specific requirements, in order to get a better fit to ill-duct and reduces complications, is possible.

A parametric analysis using finite element has been conducted to determine the influence of slot length, number of circumferential slots, tube thickness and shape-factor on stent mechanical behavior, which allow eliminating the need for extensive experimental work and knowing and quantifying the influence of those factors.

The results of finite element simulations have been used, by means of least-squares fit techniques, to obtain analytical expressions for the main mechanical characteristics of the stent (Chronic Expansive Radial Force and Radial Compression Resistance) in terms of the different geometrical factors. This allows the stent geometry to be customized without launching an iterative and costly process of modeling and simulation for each case.

Keywords

Self-expanding Colonic stent, Customized parametric design, Mechanical properties, Non-linear finite element analysis, Stent design parameters, Radial force calibration.

1. Introduction

Large bowel cancer is the most common in the digestive system. Colorectal cancer is the third most common cancer in men and the second most common in women. It is the third malignant tumor in incidence and forth in mortality in the world, after lung cancer [1] (Fig. 1). Due to its endoluminal growth to 29% of patients with this tumor developed intestinal obstruction [2].

Colonic occlusion presents the first reason for emergency colorectal surgery [3]. Traditional treatment of colonic obstruction is surgery. However, possibilities of surgery are limited, especially when it comes to elderly patients with associated serious diseases, causing high morbidity and prolonged hospitalization and a mortality rate of between 5 and 11% [4]. Moreover, in many cases it is not possible to restore intestinal continuity, so the patient is left with a permanent colostomy, with the consequent deterioration in their quality of life [5].

Sixty percent of patients with colorectal cancer present with a tumor in the left colon, and up to 25% have complete or partial occlusions at the time of diagnosis [6]. As it is well known metallic self-expanding stents are an option widely used to treat acute obstruction of colon, either for palliation or bridging or transition to surgical intervention, thus avoiding emergency surgery rates of morbidity and mortality, greater than 30% [6]. The stent allows decompression, the complete preparation of the colon and resection surgery in one step [7].

Although the placement of colonic stents is much less invasive, morbidity can be high due to the complications associated with this procedure. To prevent or minimize the complications (perforation, wrong positioning, migration and re-obstruction), it is necessary to make a correct choice of stent to use [8]. Since the technical success of a stent for a particular obstructive lesion depends mainly on its mechanical behavior, mechanical modeling is required to design the stent structure through a predictive model as does Kim et al [9] for braiding stents and Tzamtzis et al [10] for an aortic valve. This will allow custom design stents for each type of obstruction and patient.

Colon stents were introduced in the early 90s. In 1990 Dohmoto et al [11] present the treatment of a malignant rectal obstruction placing an expandable metal stent and in 1994, Tejero et al [12] reports two cases of acute malignant obstruction treated successfully with the placement of a stent prior to elective surgery. In 1996 is presented the first prototype of self-expanding colonic stent made of nitinol [13]. Since then, the field of colorectal stent placement has evolved substantially with the introduction of new stent models and more versatile deployment systems. Self-expandable metallic stents (SEMSs) are widely used to treat malignant colonic obstruction [14].

Stents design principally has two different manufacture strategies: braided or knitted wire-based stents, and tube-based stent designs [15] to which a laser cuts are practiced and shaped until its final-repose configuration. They can also be classified according to whether covered or uncovered. Although the tendency is to design them covered to prevent tumor growth and thus reduce the risk of restenosis, in practice they have not shown clear advantages over other [16]. Tumor ingrowth occurred more frequently in the uncovered group, while late migration is more common in the covered stents. In

[17] reported an increase of late migration (40%, P=0.005) and greater loss of stent function (60%, P=0.0018) with covered stents.

Different designs of colorectal stents are available for clinical use. The characteristics of some of the most extended and used like Ultraflex®, Wallstent® and colonic Wallflex® are included in Table 1. However, to the authors' knowledge, in literature no quantitative data may be found to characterize the behavior of the different types of colonic stents. A small number of studies have investigated the influence of design parameters for helical coils [18] and braided stents [9, 19] on the mechanical behavior. Experimental bench testing to understand the properties of self-expandable metallic stents for different biliary and airway endoprosthesis have been reported [20, 21]. Finite element analysis is commonly used in contrasting the main mechanical parameters (radial and axial strength, flexibility, etc.) of different stents [22-26].

This study employs a finite element (FE) approach in order to get a simulated bench testing data (Radial Compression Resistance and Chronic Radial Expansion Force) to develop a methodology for the design of customized self-expandable NiTi colonic stents adapted to each patient-specific case, taking like base a laser cutting tube stent design, by controlling geometry parameters. Finite element simulations are used to analyze the behavior of a predefined set of geometric configuration in order to establish an extrapolation technique that allows designing new stents adapted to the requirements of individual specific patients.

Table 1
Main available commercial colorectal stents [27].

Stent name	Material	Length(mm)	Diameter flare (mm)	Diameter body (mm)	Manufacturer
Ultraflex precision colonic stent®	Nitinol	57, 87, 117	30	25	Boston Scientific
Wallflex Colonic TTS®	Nitinol	60,90,120	25	22 or 25	Boston Scientific
Wallstent Enteral TTS®	Elgiloy	60,90	NA	20 or 22	Boston Scientific
Colonic Z stent®	Stainless steel	40, 60, 80, 100, 120	35	25	Wilson-Cook
Niti-s Colorectal stent®	Nitinol	60,80,100 Covered, uncovered	28-30	20, 22, 24	Taewoon-Medical Co., Ltd.
TTS Niti-s Colorectal stent®	Nitinol	60,80,100	28	20	Taewoon-Medical Co., Ltd.
Hanarostent colorectal®	Nitinol	Covered: 60, 90, 110, 130	NA	18, 22	MI Tech Co. Ltd.
		Uncovered: 80, 110, 140	NA	18, 22	

NA=not available.

2. Material and Methods

2.1. Stent model

The geometric typology used in this study is a tube-based stent with closed diamond-shaped cells (Palmaz-Schatz type), which correspond to basic geometry module used by the authors to design and manufacturing a prototype of colonic stent [28, 29]. In previous comparative analysis of stents for treatment of colorectal obstruction [29] and

by means of experimental animal testing [30], it was shown that stents based on closed cells with arms joined by rigid nodes develop higher radial force response, necessary for reopening occlusive colonic strictures where greater strength is required.

The geometrical pattern adopted allows manufacturing the initial shape preformed by cutting laser technique, creating a longitudinal nonhomogeneous distribution of grooves on the tube surface, with a given width and length. In next step the slotted tube is expanded until it reaches the stent configuration [28]. The chosen design allows a precision manufacturing process for obtaining controlled custom designs for each pathology and patient in an efficient and economically viable manner. The repose shape obtained after subsequent shaping process, thermo-mechanical treatment (numerically: stress field to zero) and electropolished [28] (Fig. 2), gives a bell-shaped profile similar to commercial device Medtronic-CoreValve used on treatment of aortic valves.

The stent is composed of a set of rings closed cells with a diamond shape, joined together by rigid joints. By setting for each stent a constant number of circumferential cells, is possible obtain areas with different stiffness varying the pattern cut along the longitudinal axis, and adjusting the expansion ratio factor imposed on each ring of cells until it gets to the desired shape.

Acting over these two design parameters, a shape-profile with longitudinally variable radial strength to facilitate optimal adaptation to the duct walls and prevent migration risk can be set [30]. The pressure exercised against duct walls by each annular cell may be adjusted independently of the profile adopted to avoid migration. So it is possible to obtain a stent with a shape adapted to each type of stenotic duct and variable radial stiffness according to the needs of each patient and pathology.

2.1.1. Parametrized geometry

Adjustment parameters for calibrating the stent design to the particular needs of each patient are the following (Fig. 3): diameter and thickness of the initial tube, number of circumferential grooves, width and length groove and size of the solid regions between slots. These parameters determine the initial preformed shape from which after expansion by mandrels and heat treatment fix the final stent geometry. In the shaping phase, the control parameter is the groove angle obtained imposing permanent deformation to each ring, hereinafter referred as *shape factor* (Fig. 3c).

Parameters that are kept constant, based on previous studies [30], are:

- *Outer tube diameter* (4.5 mm): nominal raw tube diameter before shaping process.

- *Slot width* (0.1 mm): laser-cut width produced on the original tube.

- *Hinge solid regions:* regions between adjacent lattice cells. In the proposed design they are kept constant in all cases, with a value of 0.5 mm.

- *Bevel ratio edge of slot*: models contemplated rounding corners grooves made by laser cutting; in the proposed design, the fillet radius is set to 30% of the groove width (0.03 mm).

Variable parameters defining the specific geometry of each stent and cell are:

- *Slot length (l_s, 8-18mm)*: length of the laser cut made in longitudinal direction on the original tube.

- *Number of circumferential slots (n_{cs}, 24-48)*: number of cells composing each ring.

- *Thickness (t, 0.4-0.1mm)*: wall thickness of the tube used, which corresponds with the height of the arm section of each cell.

- *Shape factor (α°):* indicates the degree of opening of each circumferential groove with respect to the horizontal (Fig. 3). For a same shape factor and different circumferential length or number of slots, it involves variation in the expansion ratio.

Table 2
Geometric parameters common to all tested configurations

Parameter	Value
Outer tube diameter (D_o)	4.5 mm
Hinge solid region (w_h)	0.5 mm
Slot width (w_s)	0.1 mm
Bevel ratio edge of slot (% of w_s)	30%

Table 3
Configurations used in finite element analysis. Variable factors to adjust mechanical response: l_s is slot length, n_{cs} the number of circumferential slots and t the wall thickness of the tube. Length of lattice unit cell is $l_s + w_h$ and each model ring has n_{cs} / 2 unit cells.

Model	l_s [mm]	n_{cs}	t [mm]
Stent 1-8	**8**	36	0.4
Stent 1-10	**10**	36	0.4
Stent 1-12 *	**12**	36	0.4
Stent 1-16	**16**	36	0.4
Stent 1-18	**18**	36	0.4
Stent 2-24	12	**24**	0.4
Stent 2-28	12	**28**	0.4
Stent 2-32	12	**32**	0.4
Stent 2-36 *	12	**36**	0.4
Stent 2-48	12	**48**	0.4
Stent 3-0.4 *	12	36	**0.4**
Stent 3-0.3	12	36	**0.3**
Stent 3-0.1	12	36	**0.1**

* reference geometry configuration (Stent 1-12= Stent 2-36= Stent 3-0.4)

In order to determine the influence of the four parameters (*ls, n_{cs}, t, α°)* used to adjust the working diameter and the mechanical response exerted on the wall duct a virtual testing battery is done. The values of constant factors common to all models simulated are included in Table 2. The values of variable factors are included in Table 3. In the case of l_s and $n_{cs,}$ ranges have been set to values which allow generate a structure of

rhomboidal mesh with a permeability to avoid as far as possible the direct intrusion of tissue from the wall of the colon, and to facilitate the development of an expansion force distributed around the whole perimeter avoiding the appearance of critical points where exerted forces would be applied in small areas of duct tissue. The adopted range of values are based in previous studies carried out by the authors [29, 30], both by FE simulations and experimental testing. The range for *t* (thickness) is determined by the common values that provide the leading manufacturers of NiTi tubes.

2.1.2. Finite Element models development

A specific tool was developed to modify geometrical parameters and get a controlled mapped mesh, element shape and size, discretizing all the entities in each customized model. A parametric model of the stent was developed writing scrip files in Python language inside the pyFormex open source code [31]. The nodes and elements of the tube are extracted in a text file which can be used in external FEA programs (Abaqus 6.11 in the present work). All models were meshed using BRICK (C3D8) and WEDGE (C3D6) elements, with linear interpolation (Fig. 4). Both the cylindrical surfaces used to conform the stent, as the used for expansion-compression simulations are meshed with four-node surface elements (SFM3D4) that allow applying radial displacement, in such a way that nodes behave like a rigid surface with continuum evolution of its shape (Fig. 4).

A sensitivity analysis was performed to determine the minimal size mesh required for an accurate simulation. For this purpose, a mesh refinement was performed in order to achieve a convergence towards a minimum of the potential energy, with a tolerance of 1% between consecutive meshes. Moreover, the same criterion was applied to stresses and strains.

2.1.3. Material behavior modelling

Nitinol is a superelastic alloy which is capable of reaching strain up to 8% without yielding, allowing a complete elastic recovering. That property makes it possible to design stents which present a soft Chronic Expansive Force (CEF), allowing a gradual relaxation of the constriction, and a high Radial Compression Resistance (RCR), which prevents the stent collapse due to external actions. In order to simulate the material behavior, a phenomenological constitutive model was used, based on the formulation developed by Auricchio and Taylor [32, 33]. To this respect the material was modeled in Abaqus 6.11 as an embedded user material subroutine (UMAT).

The alloy used for manufacturing the stent corresponds to a NiTi alloy (50.8 at% Ni, 49.2 at% Ti) supplied by Memory Metalle GmbH (Germany). A battery of six uniaxial tensile tests were performed by means of a universal machine test Instron 5565, using standard specimens obtained from sheets 1 mm thick. Every test was done considering complete loading and unloading with displacement control. The tests were performed at a reference temperature T_0= 22ºC. Fig. 5 shows the average curve of the tensile tested samples versus strain-stress curves resulting from uniaxial virtual test simulated and adjusted using the material subroutine implemented in Abaqus 6.11 code for T_0= 22ºC and T_w=37 ºC, respectively. Thermo-mechanical parameters, necessary to obtain the material behavior at body temperature T_w=37 ºC, were retrieved from literature [34].

Table 4 includes NiTi material mechanical properties fit to average values obtained from experimental testing.

Table 4
NiTi material parameters defining constitutive stress-strain curve of the alloy used in the present study. The loading and unloading rate of change of plateau with the temperature C^{AM} and C^{MA} were obtained from literature [34].

Parameter	Description	Value
E_A	Austenite elasticity module	52650 MPa
ν_A	Austenite Poisson's ratio	0.33
E_M	Martensite elasticity module	38250 MPa
ν_M	Martensite Poisson's ratio	0.33
ε_L	Maximum Transformation strain	6%
σ_s^{AM}	Start of transformation Austenite Martensite stress	385 MPa
σ_f^{AM}	End of transformation Austenite Martensite stress	460MPa
σ_s^{MA}	Start of transformation Martensite Austenite stress	200 MPa
σ_f^{MA}	End of transformation Martensite Austenite stress	180 MPa
T_0	Reference temperature	22ºC
C^{AM}	$\frac{\partial \sigma_S^{AM}}{\partial T}$	6.1 MPa/ºC
C^{MA}	$\frac{\partial \sigma_S^{MA}}{\partial T}$	6.1 MPa/ºC
$\varepsilon_{L\ Vol}$	Volumetric transformation strain	0.06

2.1.4. Stent geometry generation

A first simulation step is needed in order to get the stent configuration from the slotted tube. To this respect the slotted tube is subjected to a proportional radial expansion according to the final configuration required. Taking as reference the Stent 1-12* which is a ring of cells shaped by the expansion of an initial tube outer diameter 4.5 mm to a final outer diameter of 30.4 mm starting from a tubular preform with 36 circumferential grooves distributed uniformly with 0.1 mm width and 12 mm length, leaving a *solid hinge* between slots of 0.5 mm, it leads to an expansion ratio of 6.75 times its diameter. This is the maximum expansion to assure the integrity of the stent structure in the manufacturing process, and correspond to a *shape factor* of 24.84˚.

So, we adopted this value as the reference *shape factor* which corresponds to the maximum amplitude without reaches critical stress in any point of stent (solid hinges). Imposing the shape factor and not the final diameter allows evaluating the influence of design parameters for the maximum operating range in each configuration, therefore all the tested configurations have been shaped (by expansion) until reaching a shape factor close to 24.84˚. Table 5 shows the radial expansion imposed on each testing configuration and the shape factor reached.

Table 5
Radial expansion applied to each cutting-tube preform model to obtain a given shape factor (α°=24.84)

Model	Radial expansion enforced (mm)	D_o: Outer diameter stent after radial expansion shaping (mm)	shape factor (α°)
Stent 1-8	8.05	20.6	24.85
Stent 1-10	10.50	25.5	24.85
Stent 1-12 *	12.95	30.4	24.84
Stent 1-16	17.85	40.2	24.85
Stent 1-18	20.35	45.2	24.85
Stent 2-24	7.45	19.0	24.42
Stent 2-28	9.20	22.9	25.00
Stent 2-32	11.05	26.6	24.48
Stent 2-36*	12.95	30.4	24.84
Stent 2-48	19.10	42.7	24.55
Stent 3-0.4*	12.95	30.4	24.84
Stent 3-0.3	12.90	30.3	24.00
Stent 3-0.1	12.80	30.1	24.72

* reference geometry configuration (Stent 1-12= Stent 2-36= Stent 3-0.4)

The first step of the shaping (expansion step) was developed by deforming the stent by contact between the inner stent surface and a cylindrical rigid surface (Fig. 6a) with a variable radius during the simulation until reach the desired *shape factor*. After the expansion step, an annealing step was imposed, putting zero the stress and strain fields, simulating the thermal relaxation process and maintaining the final repose form Fig. 6b.

2.1.5. Boundary conditions

To simulate the mechanical behavior a single ring of rhombohedral cells is taken, to avoid border effects and reduce the model size. Symmetry conditions are imposed on nodes in the medial planes of each external solid hinge which link with adjacent rings. This results in a solution for the response of the entire structure at a relatively low computational expense. To avoid rigid body motions two nodes in symmetry plane are clamped in longitudinal direction (u_x=0) (Fig. 7).

2.2. Virtual radial compression-expansion test

A second simulation step is needed in order to get the mechanical behavior of the stent. To this respect, a radial compression test at 37 ° C using Abaqus/Standard v6.11 was performed. This virtual test try to reproduce as accurately as possible experimental tests which can be found in the literature [20]. In this case the diaphragm of the testing machine shown in Fig. 8a is implemented as a cylinder shaped surface meshed with three-dimensional, 4-node surface elements type SFM3D4 available in Abaqus. This surface can be deformed by imposing nodal displacements. The global behavior of cylinder resembles a rigid surface which contracts and expands according to the

boundary conditions imposed. A frictionless surface-surface contact was defined with adjustment of stent-nodes to expansion-compression cylindrical surface.

Defining the contact rigid surface-stent, radial displacements are induced as it is done in experimental trials. The cylinder is contracted to shrink the stent to the minimum size of 6 mm (18 Fr) and then is reversed the radial displacement of cylinder until the ring cells stent reaches full release.

Assessing nodal reactions on cylindrical surface, the general Chronic Radial (Outward) Force (RF) developed by each lattice ring was obtained, both in crimping and realising. This virtual trial allows obtaining the mechanical response of each lattice ring. Thus it is possible to determine the influence of each design parameter in the global response for different lattice rings. An experimental curve against a curve obtained by simulation, for a complete contraction (crimping) and expansion (releasing) process, are shown in Fig. 8. The curve obtained in the crimping process corresponds to Radial Compression Resistance (RCR) and the curve recorded during release process are defined as Chronic Radial Expansion Force (CEF).

The simulation cycle is included in Fig. 9. Similar simulated bench testing may be found in [22] and [35] applied to balloon expandable coronary stents, and in [23] to self-expanding tracheobronchial stents.

3. Results

By evaluating the radial reactions resultant on compression-expansion cylindrical surface, the characteristic curves are obtained for each of the lattice rings which conforms the stent. These curves have been evaluated for every configuration considered in the study, according to the different variable parameters (Table 3).

Because the material exhibits different behavior in loading and unloading, the radial force exerted by the device presents also a compression path (RCR) and another of release (CEF) (Fig. 8b, d).

Although both magnitudes are necessary from a point of view of stent design, in terms of clinical application the CEF magnitude defines the force exerted by stent against the treat duct driving the walls tissue until reach the desired lumen. So we can define the working range of a stent as the diameter range where it is able to keep a CEF within a tolerance around a nominal value, which corresponds with the central plate present in all curves obtained. Thereby, the mean value of the plate at CEF curve defines the nominal force of each stent configuration. The RCR magnitude is also essential in order to prevent the collapse of the stent once implanted, when it is subjected to pressures generated by peristalsis or any other kind of external compressive load.

The evolution of the RCR curve may be seen in Fig. 8d, which presents an upper plate to CEF curve. The mean values of RCR for each simulation case are plotted in top right corner in Fig. 10. For clarity and brevity in sections 3.1 to 3.3 only CEF is referenced; however both values of CEF and RCR from all simulations carried out have been used to adjust the behavior surfaces (section 3.4) (dots plotted on Fig. 14).

3.1. Influence of slot length (l_s)

The influence of slot length is determined based on stent configurations (Stent 1-xx, Table 3) with a constant number of circumferential slots (n=36) and tube thickness (t= 0.4 mm) with the same shape factor (α˚=24.85˚). Fig. 10 shows an overlay of the CEF curves where we can see that is possible calibrate the stent's response maintaining fixed the shape factor, varying only the slot length from 8 to 18 mm. If the stent working range was defined for an inner diameter variation of duct to be treated between 10 and 18 mm, it is possible calibrating the nominal force between 10 and 25 N. But, if the working range is extended to ducts with diameters larger than 30 mm, the use of slot lengths less than 12 mm would be discarded and the maximum nominal force would be limited to 16 N.

3.2. Influence of the number of circumferential slots (n_{cs})

The influence of the number of circumferential slots has been based on the simulations performed for configurations (Stent 2-xx, Table 3) where slot length and tube thickness has been remained constant to 12 mm and 0.4 respectively, and the shape factor close to the reference value of 24.85˚ (Table 5).

Fig. 11 shows an overlap of the CEF curves where is possible see that we can calibrate the response of the lattice ring maintaining a constant shape factor, and varying only the number of circumferential grooves for a given working range.

In the cases shown in Fig. 11, for an operating range from 10 to 18 mm the force exerted can be calibrated between 10 and 40 N by varying the number of circumferential grooves 24 to 48. But, for ducts with diameters around 25 mm, the number of slots must be greater than 32 and the maximum nominal force would be limited to 21 N.

3.3. Influence of the tube thickness (t)

Keeping constant the number of circumferential grooves to 36 and the slot length to 12 mm and without changing the shape factor, different wall tube-stent thicknesses were tested (Stent 3-xx, Table 3), obtaining the curves for Chronic Radial Expansion Force (CEF). By overlapping virtual testing data in the same graph (Fig. 12), it was found that the operating range of duct diameter is between 12 and 26 mm and the radial force exerted between 6 and 16 N, depending on tube thickness.

3.4. Interpolated surfaces for stent behavior

Processing the results of all simulations it is possible to get analytical expressions which describe the *Chronic Radial Expansion Force* (CEF) and the *Radial Compression Resistance* (RCR), respectively, exerted by the stent depending on the considered

parameters: slot length (l_s), number of circumferential grooves (n_{cs}) and wall tube-stent thicknesses (t).

The general equation considered for the behavior surface corresponds to a two variables polynomial function of order n=4, as follows,

$$f_i(x,D_S) = C_0 + C_1 \cdot x + C_2 . \cdot D_S + C_3 \cdot x^2 + C_4 \cdot x \cdot D_S + C_5 \cdot D_S{}^2 + C_6 \cdot x^3 + C_7 \cdot x^2 \cdot D_S + C_8 \cdot x \cdot D_S{}^2 + C_9 \cdot D_S{}^3 + C_{10} \cdot x^4 + C_{11} \cdot x^3 \cdot D_S + C_{12} \cdot x^2 \cdot D_S{}^2 + C_{13} \cdot x \cdot D_S{}^3 + C_{14} \cdot D_S{}^4 \quad (1)$$

where f_i represents expression for CEF obtained adjusting data from release step or RCR using data from crimping step, x is the respective design parameter which may be l_s, n_{cs} or t, and D_S the outer stent diameter. The least squares technique was used to calculate the polynomial coefficients (

Table 6). The fitting accuracy was tested by calculating the Pearson correlation coefficient R^2.

Table 6
Coefficients of the behavior fit-function, where l_s [mm] is the slot length, n_{cs} the number of circumferential slots, t [mm] the tube thickness, CEF the Chronic Radial Expansion Force and RCR the Radial Compression Resistance**.**

$f_i(x,D_S)$						
	CEF			**RCR**		
Design variable:	**$x=l_s$**	**$x=n_{cs}$**	**x=t**	**$x=l_s$**	**$x=n_{cs}$**	**x=t**
Coefficients	[mm]		[mm]	[mm]		[mm]
C_0	330.0000	683.4000	35.6500	100.9000	482.8000	21.7800
C_1	-59.3600	-37.7900	51.7400	-1.5080	-24.6700	32.1800
C_2	-20.5200	-45.9600	-6.4780	-6.5410	-17.5100	-3.4780
C_3	4.5560	0.5460	0.0000	-1.3300	0.3175	0.0000
C_4	2.8570	1.9190	-0.2601	1.6940	1.3100	4.9710
C_5	0.3785	1.3180	0.3840	-0.3001	-0.5182	0.2173
C_6	-0.1209	-0.0772	--	0.0692	-0.0001	--
C_7	-0.2808	0.0897	--	-0.0764	-0.0195	--
C_8	0.0817	-0.0798	-0.0377	0.0165	0.0105	-0.1948
C_9	-0.0304	-0.0134	-0.0070	--	--	-0.0042
C_{10}	--	3.8E-05	--	--	--	--
C_{11}	0.0100	0.0015	--	--	--	--
C_{12}	-0.0056	-0.0020	--	--	--	--
C_{13}	0.0017	0.0011	--	--	--	--
C_{14}	-9.8E-06	--	--	--	--	--
R^2	0.9264	0.9283	0.9632	0.9124	0.9239	0.9754

The fitted surfaces are plotted in Fig. 13 and Fig. 14 together with the discrete values obtained from parametric FE simulations.

3.5. Design of a customized stent

Based on the parametric study data and using the mathematical expressions obtained which characterize numerically the influence of each design factor (behavior surfaces), we can calibrate stent in an efficient way to the specific requirements.

As an example, a distribution of estimated required net radial forces is presented in Fig. 15 in three different areas of the same acute stenosis which by surgical prescription are considered suitable for restore transit on the section of affected colon. Those values might be estimated by balloon catheter via colonoscopy in subacute strictures; performing a minimal local stricture dilatation and recording the pressure to inflate the balloon, an estimation of radial force need in each area could be obtained.

Among the different possibilities (i.e., single solution doesn't exist), varying the length slots and keeping the rest of the parameters constant (including *shape factor*), for example, the stent configuration can be obtained. The preliminary dimensioning of geometry gives rise to a cutting pattern as illustrated in Fig. 16a, with zones 1-3 with slot length according the given specifications and a transition zone 4. After forming process simulation, the stent configuration shown in Fig. 16b is obtained.

In view of the obtained results, this study provides behavior surfaces expressions that make possible to determine the value of the chosen design variables depending of diameter and radial force required in each stent zone, so it is possible obtaining a customized stent design with different stiffness areas, adapted to the patient specific needs.

4. Discussion and conclusions

Expandable metallic stents was shown to be a safe, easy, and effective technique as a bridge to surgery and palliative treatment of colorectal cancer and associated with an acceptable complication rate. The most serious complication is the perforation, to avoid it is important to make a correct indication and choice of stent [8]. Other complications include stent migration and reobstruction [36-40].

Concerning the risk factors associated with complications, complete colorectal obstruction and the use of covered stents contribute to the complications [41]. The degree of occlusion has been reported to be one of the important risk factors, especially because a total obstruction may be associated with friable and damaged tissue [42]. Furthermore the length of the obstruction and the presence of distal angulations are poor prognosis factors [43].

To avoid complications is essential to know the pathology of tumor stenosis, this includes 3 areas: the most stenotic tumor area where there has been obstruction, tumor mass that precedes and follows the proper obstructed area, and part of anterior intestine and distal, which usually has a significant edema. It is therefore necessary to adapt the design of the stent to the different areas that make up an anatomical area affected by the

obstructive tumor, and the peristaltic movement of the intestine that precedes and continues to the tumor area, as the technical success of a stent depend directly on mechanical behavior, which can be estimated through predictive simulation model by FEA [22-26, 44-47] or experimentally like in Isayama et al [20] and Rebelo et al [48] for a braiding stent.

While stents work well in the vascular structures, biliary track or ureter, its operation is more difficult in the colon, because of the special peristalsis and fecal content characteristics, favoring its displacement or obstruction. Severe complications occur in up to 10% of patients. These consist of stent migration, perforation, and sepsis. Stent migration rates range between 10 and 12%. Migration can happen a few days after stent deployment or later in the disease course. These were probably a result of tumor shrinkage from adjuvant chemotherapy [40] or to the effect of intestinal peristalsis. A complete study about stent migration and colon perforation can be found in [49].

In the present work, FE analysis has been used to analyze influence of several design parameters on global behavior of a given stent geometry. The proposed design allows a customized stent manufacture. And make possible the adaptation of endoprosthesis to the particularities of each case to be treated. So we can decrease the contact radial force in the healthy parts of the colon while in stenotic zone the radial expansion reaction may be higher.

The parametric study of the proposed geometry makes it possible to have a good approximation of the mechanical behavior of the stent. The main geometric parameters of the stent can be quickly obtained using the analytical expressions according to a variable stiffness profile required for each case: The main mechanical characteristics, Chronic Radial Expansion Force (CEF) and Radial Compression Resistance (RCR), can be also assessed for the diameter range, and they could aid in the calibration of customized stent designs.

Of the three parameters used to calibrate the response of the stent, and in view of the results obtained, variations in the thickness of the tube in the usual ranges provided by manufacturers (400 to 300 μm) produce minimal variations of CEF nominal force (9%); for higher variations of CEF much lower thicknesses should be used. On the other hand, the manufacturing on demand of tubes with different thickness implies high economic and temporal costs. On the contrary, the use of parameters L_s and n_{cs} allows adjusting the pattern shape in the own manufacturing site and obtaining a wider set of mechanical responses for any working range.

For the number of slots n_{cs}, inside the analyzed range, values below 24 generate very coarse lattices that produce problems of high pressures in the tissue and even its possible intrusion, and values above 48 lead to too thin struts at stent structure, with crushing risk under peristaltic movement pressures. The slot length l_s appears as the most flexible and effective design parameter.

A wide range of constant recovery force is a key factor achieving stent functionality; the customized stents offer the advantages to adjust the recovering force depending on the clinical requirements.

An essential topic in colorectal stents concerns the strain and stress values reached in the stent with the maximum peristaltic compression, capable to cause the stent crushing [30]. The superelasticity of NiTi alloys is a good ally to support this kind of loads, avoiding the strain values reached the elastic limit, so no yielding occurs. However, it is necessary a good dimensional calibration to ensure that the lattice structure develop enough radial force to recover the previous stent-duct equilibrium stage guaranteeing a proper intestinal transit. So the RCR magnitude is essential in order to prevent the collapse of the stent once implanted, when it is subjected to pressures generated by peristalsis or any other kind of external compressive load.

Despite the clinical studies concerning application of colonic stents [13-16], no comparative studies of colonic stent behavior using FE simulations have been found.

The results of the study show that NiTi self-expanding bell-shaped customized stent may be an effective alternative to relieve colonic obstruction, either as a bridge to elective single-stage surgery avoiding a stoma, or as a definitive palliative solution in patients with irresectable tumor or poor estimated survival.

The use of the behavior surfaces expressions obtained allows determining the value of the chosen design variable (usually *ls*) depending of diameter and radial force required in each stent zone, so is possible obtain a customized stent design with different stiffness areas in a direct and simple way, without additional simulations. In summary, this study provides significant new insights for the customized design of colonic stents, giving guidance on design features to optimize the design-manufacture process.

Conflict of interest statement

The authors have no professional or financial conflicts of interest to discloser.

Acknowledgments

The authors acknowledge Beatriz Garcés for his collaboration performing preliminary simulation tests.

This research did not receive any specific grant from funding agencies in the public, commercial, or not-for-profit sectors.

References

[1] J. Ferlay, I. Soerjomataram, R. Dikshit, S. Eser, C. Mathers, M. Rebelo, D.M. Parkin, D. Forman, F. Bray, Cancer incidence and mortality worldwide: sources, methods and major patterns in GLOBOCAN 2012, Int J Cancer. Journal international du cancer 136(5) (2015) E359-86.

[2] G.T. Deans, Z.H. Krukowski, S.T. Irwin, Malignant obstruction of the left colon, Brit J Surg 81(9) (1994) 1270-6.

[3] R. Frago, E. Kreisler, S. Biondo, E. Alba, J. Domínguez, T. Golda, D. Fraccalvieri, M. Millán, L. Trenti, Complications of Distal Intestinal Occlusion Treatment With Endoluminal Implants, Cir Espan 89(7) (2011) 448-455.

[4] C.S. McArdle, D.J. Hole, Emergency presentation of colorectal cancer is associated with poor 5-year survival, Brit J Surg 91(5) (2004) 605-9.

[5] S. Biondo, J. Martí-Ragué, E. Kreisler, D. Parés, A. Martín, M. Navarro, L. Pareja, E. Jaurrieta, A prospective study of outcomes of emergency and elective surgeries for complicated colonic cancer, Am J Surg 189(4) (2005) 377-83.

[6] S. Adamsen, S. Meisner, Expandable metal stents for malignant colorectal obstruction, Tech in Gastrointest Endosc 3(2) (2001) 103-107.

[7] R. Castaño, J.D. Puerta, O.a. Alvarez, J. Lopera, E. Sanin, F. Erebrie, E. NuñEz, L.E. GarcíA, Self-Expanding Metal Stents in Malignant and Benign Colonic Obstructions, Gastrointest Endosc 67(5) (2008) AB151.

[8] N. Srinivasan, R.A. Kozarek, Stents for colonic strictures: Materials, designs, and more, Tech in Gastrointest Endosc 16(3) (2014) 100-107.

[9] J.H. Kim, T.J. Kang, W.-R. Yu, Mechanical modeling of self-expandable stent fabricated using braiding technology, J Biomech 41(15) (2008) 3202-3212.

[10] S. Tzamtzis, J. Viquerat, J. Yap, M.J. Mullen, G. Burriesci, Numerical analysis of the radial force produced by the Medtronic-CoreValve and Edwards-SAPIEN after transcatheter aortic valve implantation (TAVI), Med Eng Phys 35(1) (2013) 125-30.

[11] M. Dohmoto, K.D. Rupp, G. Hohlbach, Endoscopically-implanted prosthesis in rectal carcinoma (in German), Dtsch Med Wochenschr 115(23) (1990) 915.

[12] E. Tejero, A. Mainar, L. Fernández, R. Tobío, M.A. De Gregorio, New procedure for the treatment of colorectal neoplastic obstructions, Dis Colon Rectum 37(11) (1994) 1158-9.

[13] R.M. Bashir, D.E. Fleischer, T.J. Stahl, S.B. Benjamin, Self-expandable nitinol coil stent for management of colonic obstruction due to a malignant anastomotic stricture, Gastrointest Endosc 44(4) (1996) 497-501.

[14] R. Moroi, K. Endo, R. Ichikawa, H. Nagai, H. Shinkai, T. Kimura, F. Ishiyama, K. Yaguchi, S. Kayaba, T. Shimosegawa, The Effectiveness of Self-Expandable Metallic Stent Insertion in Treating Right-Sided Colonic Obstruction: A Comparison between SEMS and Decompression Tube Placement and an Investigation of the Safety and Difficulties of SEMS Insertion in Right Colons, Gastroent Res Pract (2014) 372918.

[15] D. Stoeckel, A. Pelton, T. Duerig, Self-expanding nitinol stents: material and design considerations, Eur Radiol 14(2) (2004) 292-301.

[16] Y. Zhang, J. Shi, B. Shi, C.Y. Song, W.F. Xie, Y.X. Chen, Comparison of efficacy between uncovered and covered self-expanding metallic stents in malignant large bowel obstruction: a systematic review and meta-analysis, Colorectal Dis 14(7) (2012) e367-74.

[17] K.M. Lee, S.J. Shin, J.C. Hwang, J.Y. Cheong, B.M. Yoo, K.J. Lee, K.B. Hahm, J.H. Kim, S.W. Cho, Comparison of uncovered stent with covered stent for treatment of malignant colorectal obstruction, Gastrointest Endosc 66(5) (2007) 931-6.
[18] J. Huo, R. Rojas, J. Bohlin, J. Hilborn, E.K. Gamstedt, Parametric elastic analysis of coupled helical coils for tubular implant applications: Experimental characterization and numerical analysis, J Mech Behav Biomed 29 (2014) 462-469.
[19] R. Rebelo, N. Vila, R. Fangueiro, S. Carvalho, S. Rana, Influence of design parameters on the mechanical behavior and porosity of braided fibrous stents, Mater Design 86 (2015) 237-247.
[20] H. Isayama, Y. Nakai, Y. Toyokawa, O. Togawa, C. Gon, Y. Ito, Y. Yashima, H. Yagioka, H. Kogure, T. Sasaki, T. Arizumi, S. Matsubara, N. Yamamoto, N. Sasahira, K. Hirano, T. Tsujino, N. Toda, M. Tada, T. Kawabe, M. Omata, Measurement of radial and axial forces of biliary self-expandable metallic stents, Gastrointest Endosc 70(1) (2009) 37-44.
[21] A. Ratnovsky, N. Regev, S. Wald, M. Kramer, S. Naftali, Mechanical properties of different airway stents, Med Eng Phys 37(4) (2015) 408-15.
[22] J.A. Grogan, S.B. Leen, P.E. McHugh, Comparing coronary stent material performance on a common geometric platform through simulated bench testing, J Mech Behav Biomed 12 (2012) 129-138.
[23] D.J. McGrath, B. O'Brien, M. Bruzzi, P.E. McHugh, Nitinol stent design – understanding axial buckling, J Mech Behav Biomed 40 (2014) 252-263.
[24] L. Petrini, F. Migliavacca, F. Auricchio, G. Dubini, Numerical investigation of the intravascular coronary stent flexibility, J Biomech 37(4) (2004) 495-501.
[25] F. Migliavacca, L. Petrini, M. Colombo, F. Auricchio, R. Pietrabissa, Mechanical behavior of coronary stents investigated through the finite element method, J Biomech 35(6) (2002) 803-11.
[26] F. Etave, G. Finet, M. Boivin, J.C. Boyer, G. Rioufol, G. Thollet, Mechanical properties of coronary stents determined by using finite element analysis, J Biomech 34(8) (2001) 1065-75.
[27] L. Feo, D.M. Schaffzin, Colonic stents: the modern treatment of colonic obstruction, Adv Ther 28(2) (2011) 73-86.
[28] S. Domingo, S. Puertolas, L. Gracia-Villa, M. Mainar, J. Uson, J.A. Puertolas, Design, manufacture and evaluation of a NiTi stent for colon obstruction, Bio-Med Mater Eng 15(5) (2005) 357-65.
[29] S. Domingo, S. Puértolas, L. Gracia-Villa, J.A. Puértolas, Mechanical comparative analysis of stents for colorectal obstruction, Minim Invasiv Ther 16(2) (2007) 126-36.
[30] S. Puértolas, E. Bajador, J.A. Puértolas, E. López, E. Ibarz, L. Gracia, A. Herrera, Study of the behavior of a bell-shaped colonic self-expandable NiTi stent under peristaltic movements, Biomed Res Int (2013) 370582.
[31] B. Verhegghe, pyFormex Documentation-Release 0.8.5, 2011.
[32] F. Auricchio, R.L. Taylor, J. Lubliner, Shape-memory alloys: macromodelling and numerical simulations of the superelastic behavior, Comput Method Appl M 146(3–4) (1997) 281-312.
[33] J. Arghavani, F. Auricchio, R. Naghdabadi, A finite strain kinematic hardening constitutive model based on Hencky strain: General framework, solution algorithm and application to shape memory alloys, Int J Plasticity 27(6) (2011) 940-961.
[34] F. Iannaccone, N. Debusschere, S. De Bock, M. De Beule, D. Van Loo, F. Vermassen, P. Segers, B. Verhegghe, The influence of vascular anatomy on carotid

artery stenting: a parametric study for damage assessment, J Biomech 47(4) (2014) 890-8.
[35] N. Li, H. Zhang, H. Ouyang, Shape optimization of coronary artery stent based on a parametric model, Finite Elem Anal Des 45(6–7) (2009) 468-475.
[36] S.H. Han, J.H. Lee, Colonic stent-related complications and their management, Clin Endosc 47(5) (2014) 415-9.
[37] J.D. Samper Wamba, A. Fernández Martínez, L. González Pastrana, L. López González, Ó. Balboa Arregui, Efficacy and complications in the use of self-expanding colonic stents: an analysis of 15 years' experience, Radiología 57(5) (2015) 402-11.
[38] J. Jiménez-Pérez, J. Casellas, J. García-Cano, J. Vandervoort, O.R. García-Escribano, J. Barcenilla, A.A. Delgado, P. Goldberg, F. Gonzalez-Huix, E. Vázquez-Astray, S. Meisner, Colonic stenting as a bridge to surgery in malignant large-bowel obstruction: a report from two large multinational registries, Am J Gastroenterol 106(12) (2011) 2174-80.
[39] S. Sebastian, S. Johnston, T. Geoghegan, W. Torreggiani, M. Buckley, Pooled analysis of the efficacy and safety of self-expanding metal stenting in malignant colorectal obstruction, Am J Gastroenterol 99(10) (2004) 2051-7.
[40] F. Camúñez, A. Echenagusia, G. Simó, F. Turégano, J. Vázquez, I. Barreiro-Meiro, Malignant colorectal obstruction treated by means of self-expanding metallic stents: effectiveness before surgery and in palliation, Radiology 216(2) (2000) 492-7.
[41] J.H. Choi, Y.J. Lee, E.S. Kim, K.B. Cho, K.S. Park, B.K. Jang, W.J. Chung, J.S. Hwang, Covered self-expandable metal stents are more associated with complications in the management of malignant colorectal obstruction, Surg Endosc 27(9) (2013) 3220-7.
[42] A.J. Small, N. Coelho-Prabhu, T.H. Baron, Endoscopic placement of self-expandable metal stents for malignant colonic obstruction: long-term outcomes and complication factors, Gastrointest Endosc 71(3) (2010) 560-72.
[43] D.J. Boyle, C. Thorn, A. Saini, C. Elton, G.K. Atkin, I.C. Mitchell, K. Lotzof, A. Marcus, P. Mathur, Predictive factors for successful colonic stenting in acute large-bowel obstruction: a 15-year cohort analysis, Dis Colon Rectum 58(3) (2015) 358-62.
[44] D.J. McGrath, B. O'Brien, M. Bruzzi, N. Kelly, J. Clauser, U. Steinseifer, P.E. McHugh, Evaluation of cover effects on bare stent mechanical response, J Mech Behav Biomed 61 (2016) 567-580.
[45] M. Azaouzi, A. Makradi, S. Belouettar, Deployment of a self-expanding stent inside an artery: A finite element analysis, Mater Design 41(0) (2012) 410-420.
[46] J. Huo, R. Rojas, J. Bohlin, J. Hilborn, E.K. Gamstedt, Parametric elastic analysis of coupled helical coils for tubular implant applications: experimental characterization and numerical analysis, J Mech Behav Biomed 29 (2014) 462-9.
[47] S. Tammareddi, G. Sun, Q. Li, Multiobjective robust optimization of coronary stents, Mater Design 90 (2016) 682-692.
[48] R. Rebelo, N. Vila, R. Fangueiro, S. Carvalho, S. Rana, Influence of design parameters on the mechanical behavior and porosity of braided fibrous stents, Mater Design 86 (2015) 237-247.
[49] J.H. Kim, H.Y. Song, Y.D. Li, J.H. Shin, J.H. Park, C.S. Yu, J.C. Kim, Dual-design expandable colorectal stent for malignant colorectal obstruction: comparison of flared ends and bent ends, Am J Roentgenol 193(1) (2009) 248-54.

Figures:

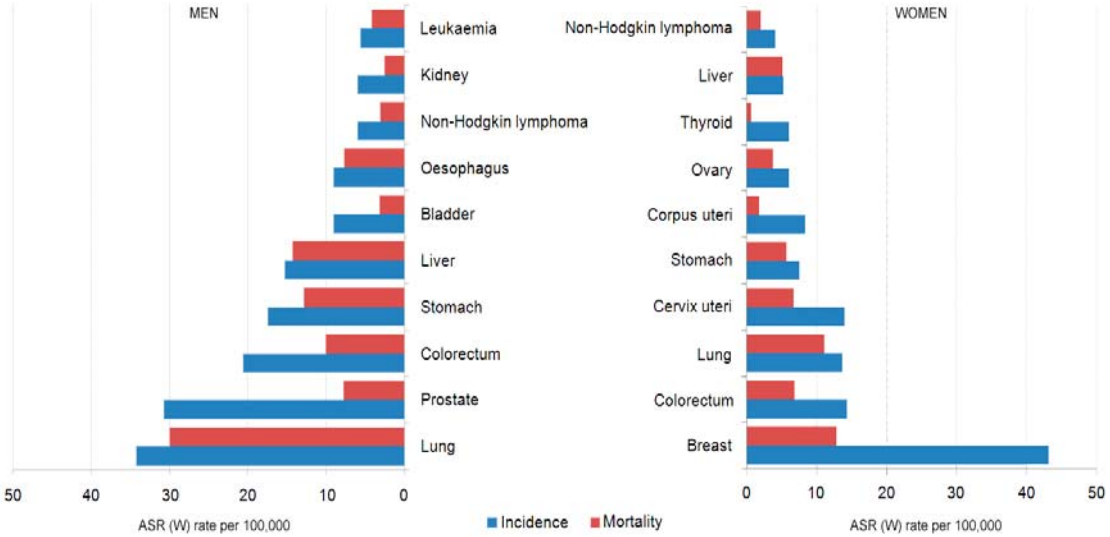

Fig. 1. Malignant tumors with the highest ratio of incidence and mortality in the world (rate per 100,000 population). [1].

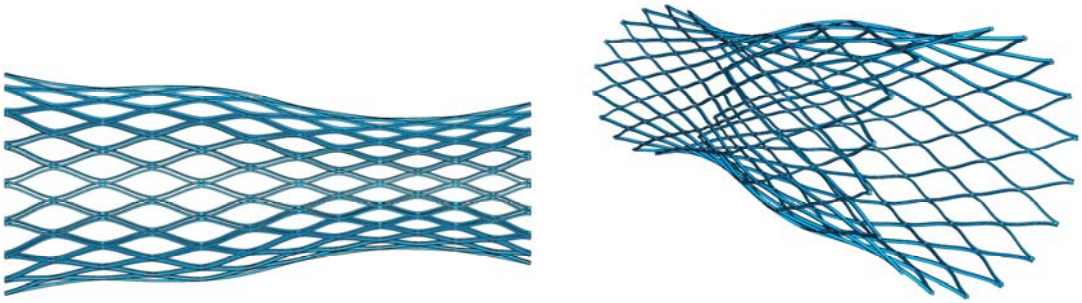

Fig. 2. Stent geometry with adapted profile and variable radial stiffness sections [30] .

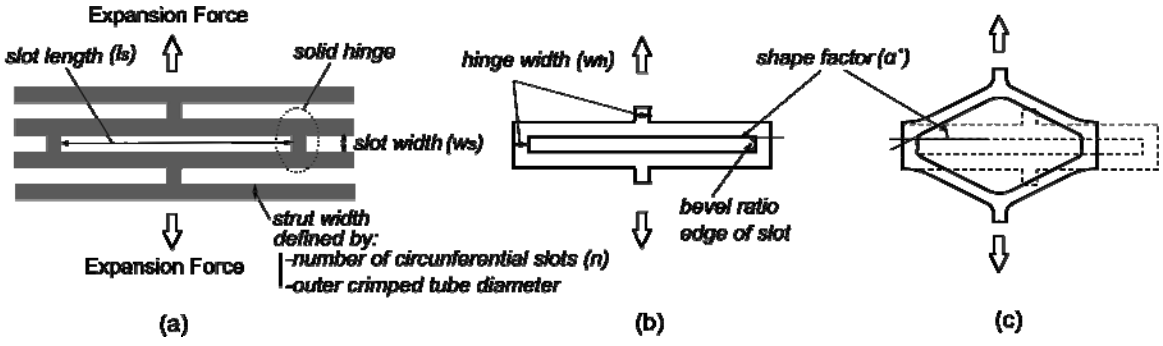

Fig. 3. (a) Scheme of perform pattern subjected to circumferential stretching; (b) crimped lattice unit cell before expansion process; (c) Diamond shape adopted after circumferential expansion, solid joints acting like hinges. The vertical arrows denote the circumferential expansion forces. The dashed lines in (c) denote unexpanded configuration of unit lattice cell to show the shortening produced and define the *shape factor* parameter.

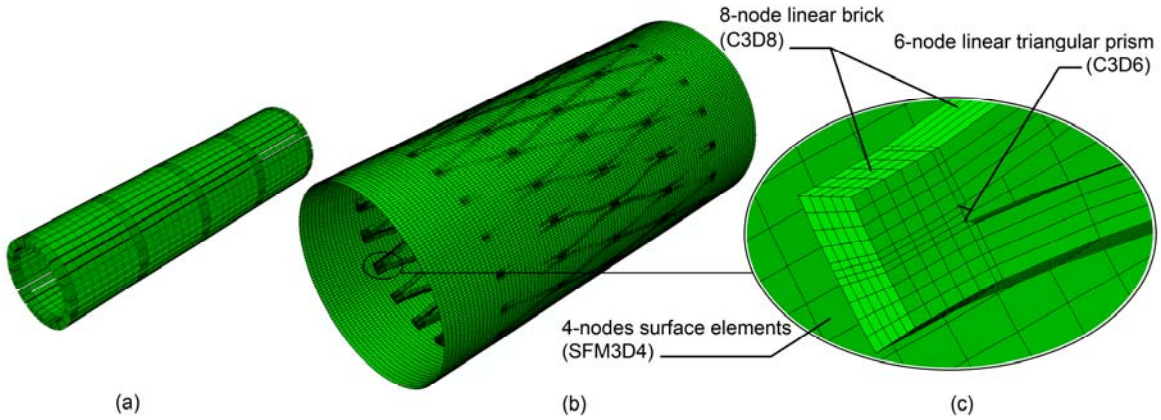

Fig. 4. Finite element model of the stent. (a) slotted tube; (b) the tubular surface model the mandrel used to get the repose stent configuration after annealing; (c) detail of mesh and elements used.

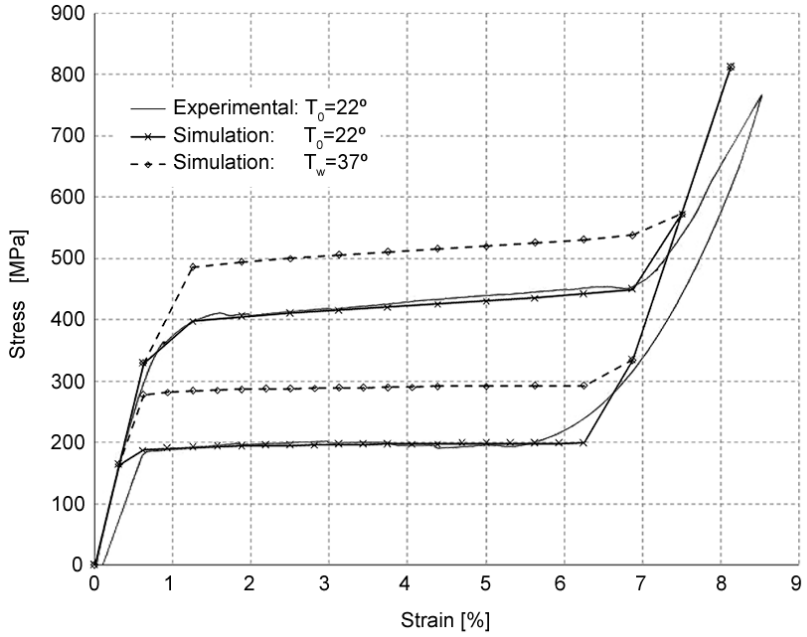

Fig. 5. Strain-stress curves of used Nitinol alloy. Experimental curve obtained from mechanical test at 22ºC, adjusted curve in Abaqus 6.11 using parameters in Table 4, and extrapolated curve at body temperature (37ºC).

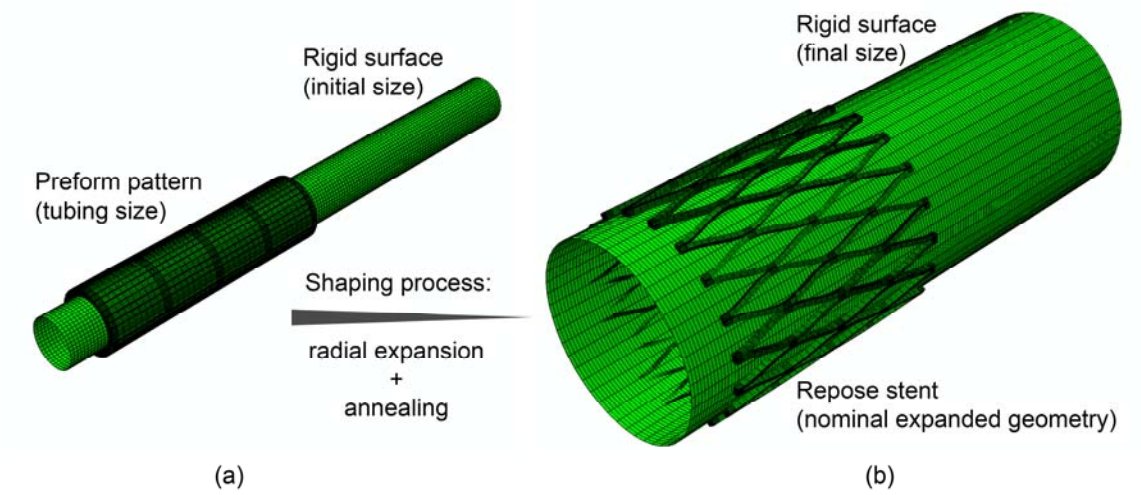

Fig. 6. Obtention of the initial stent geometry by virtual shaping simulation. a) slotted tube geometry. b) stent configuration after shaping process.

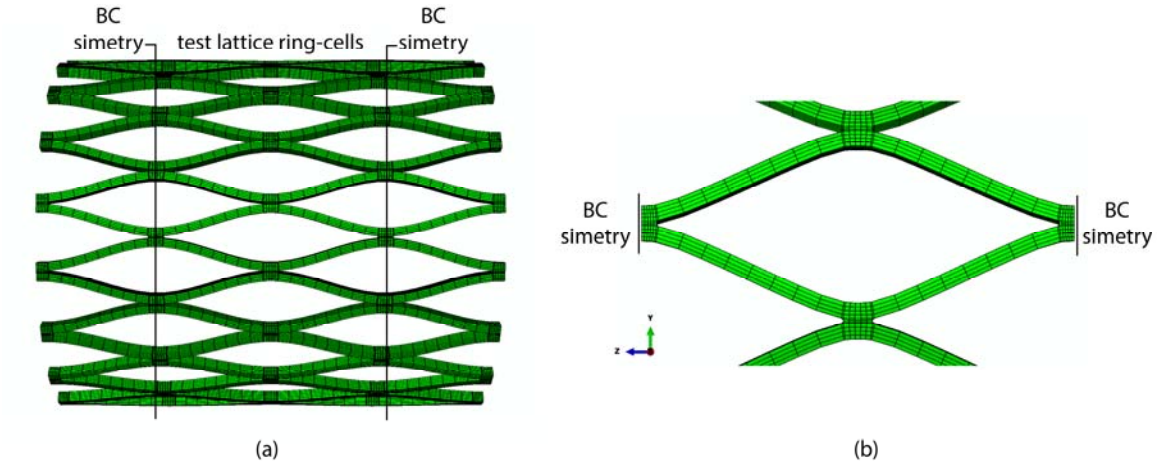

Fig. 7. Boundary conditions. a) representative field of study (test lattice ring cells); b) boundary conditions in the cylindrical coordinates system (lattice unit cell).

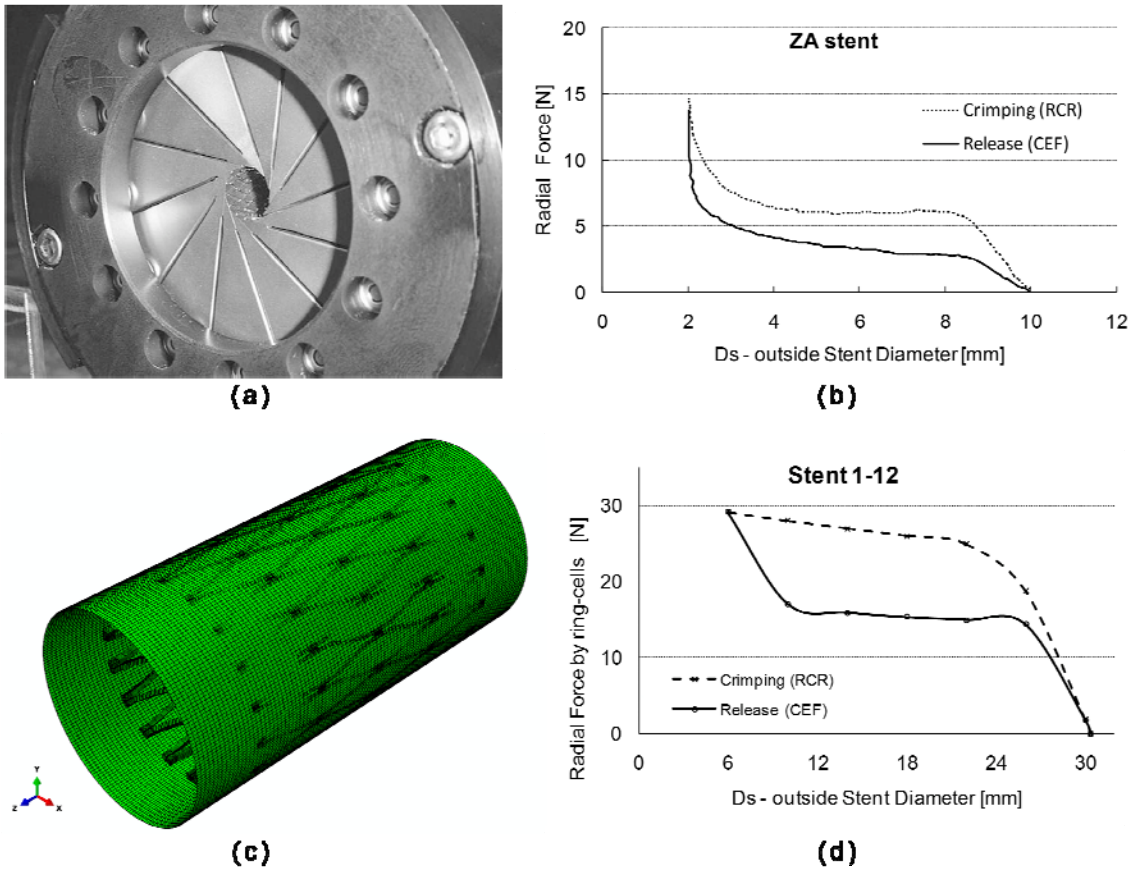

Fig. 8. Test to assess mechanical characteristics: (a) the cylinder of the RF measurement machine, RX 500, supplied by Machine Solution, Fragstaff, Arizona [20] experimental test; (b) example of experimental RF curve recorded against the diameter in expansion and contraction processes with a radial force measurement machine for a biliary NiTi stent, adapted from [20]; (c) virtual test FE model; (d) chronic radial force (RF) of the reference configuration stent 1-12 obtained by FE simulation.

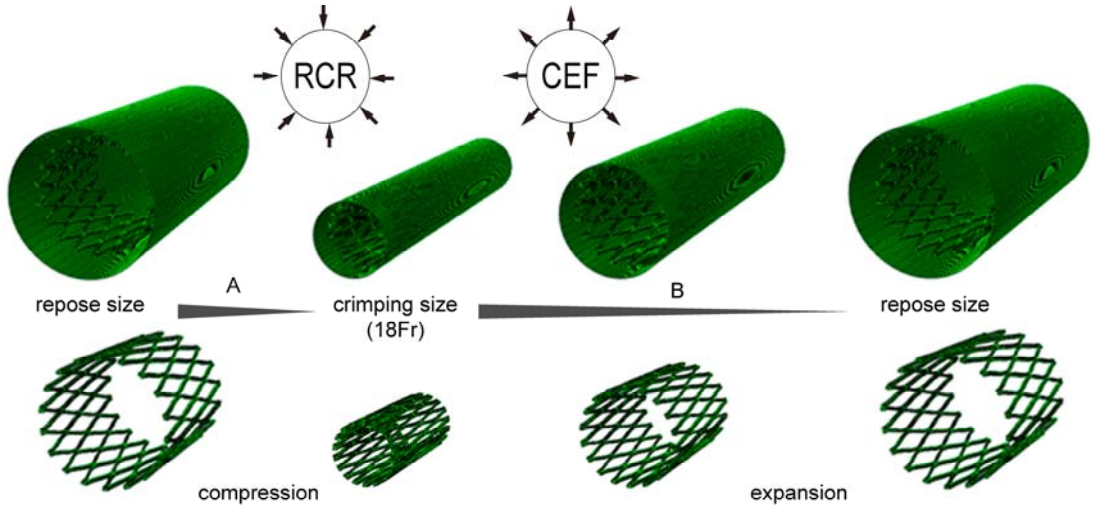

Fig. 9. Simulation cycle: A - compression until reach the maximum crimping size (18 Fr) to assess the Radial Compression Resistance (RCR); B-rigid surface expansion and stent deployment to assess the Chronic Radial Expansion Force (CEF).

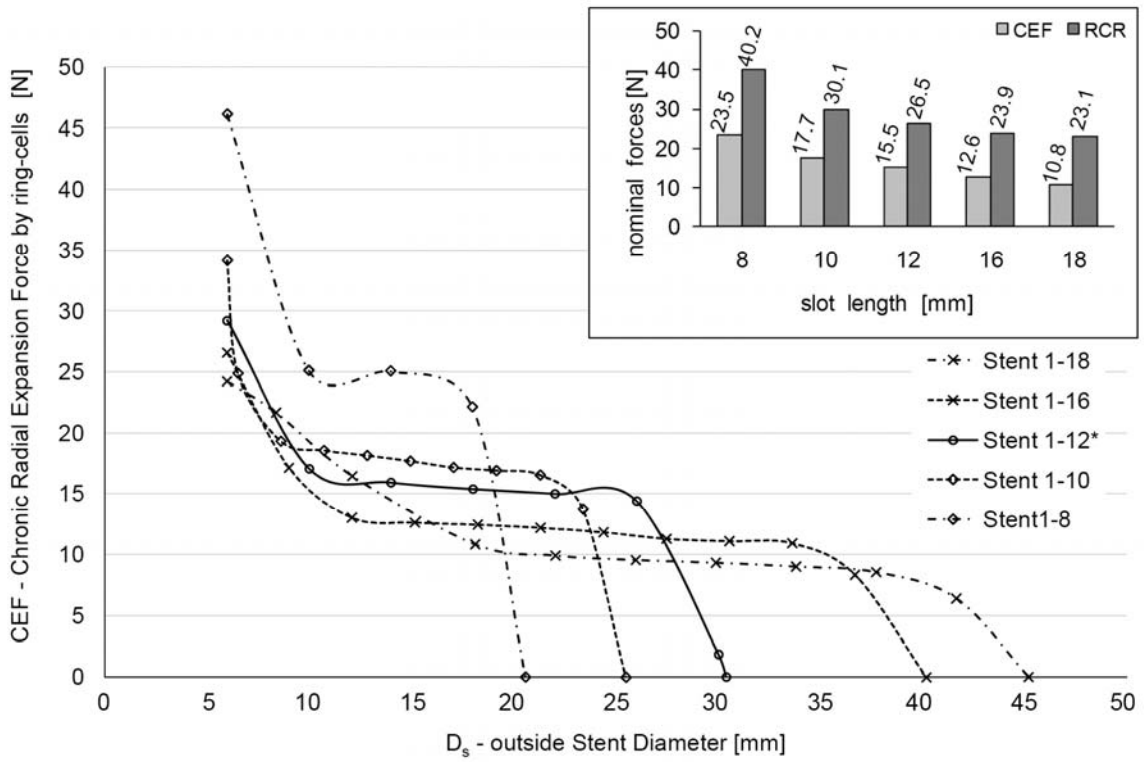

Fig. 10. Chronic Radial Expansion Force (CEF) curve for different slot length. The minimum diameter corresponds to the crimping size for a catheter of 18Fr.

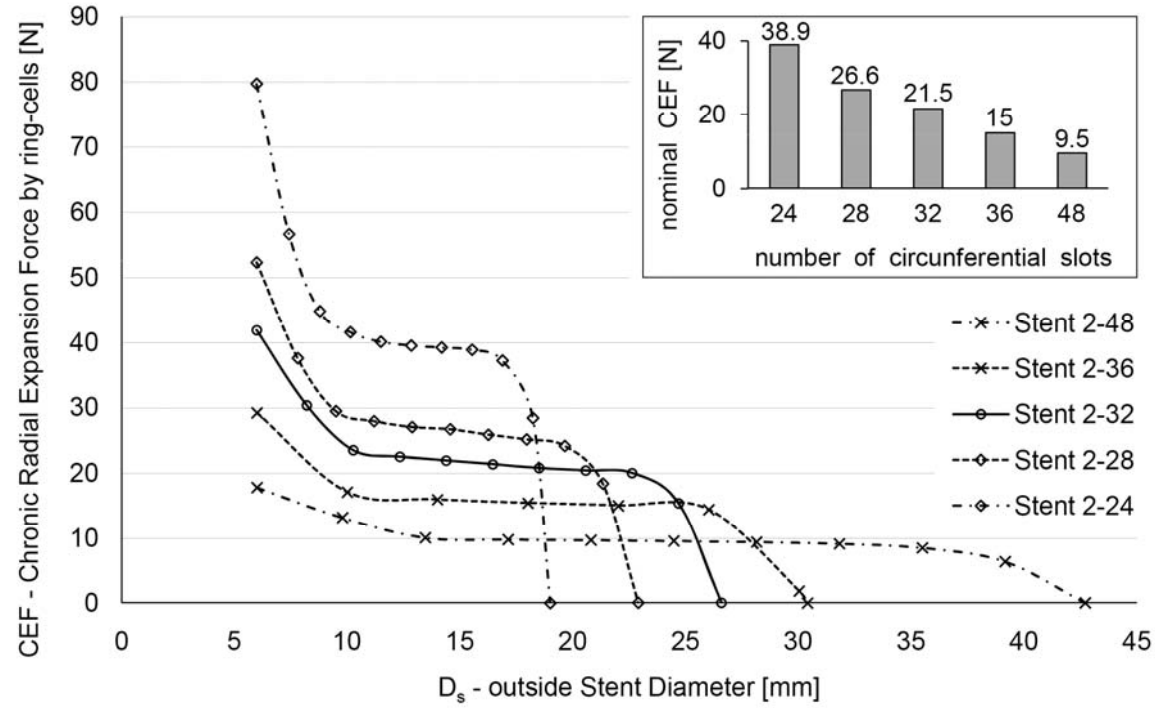

Fig. 11. Chronic Radial Expansion Force (CEF) curve for different number of circumferential slots. The minimum diameter corresponds to the crimping size for a catheter of 18Fr.

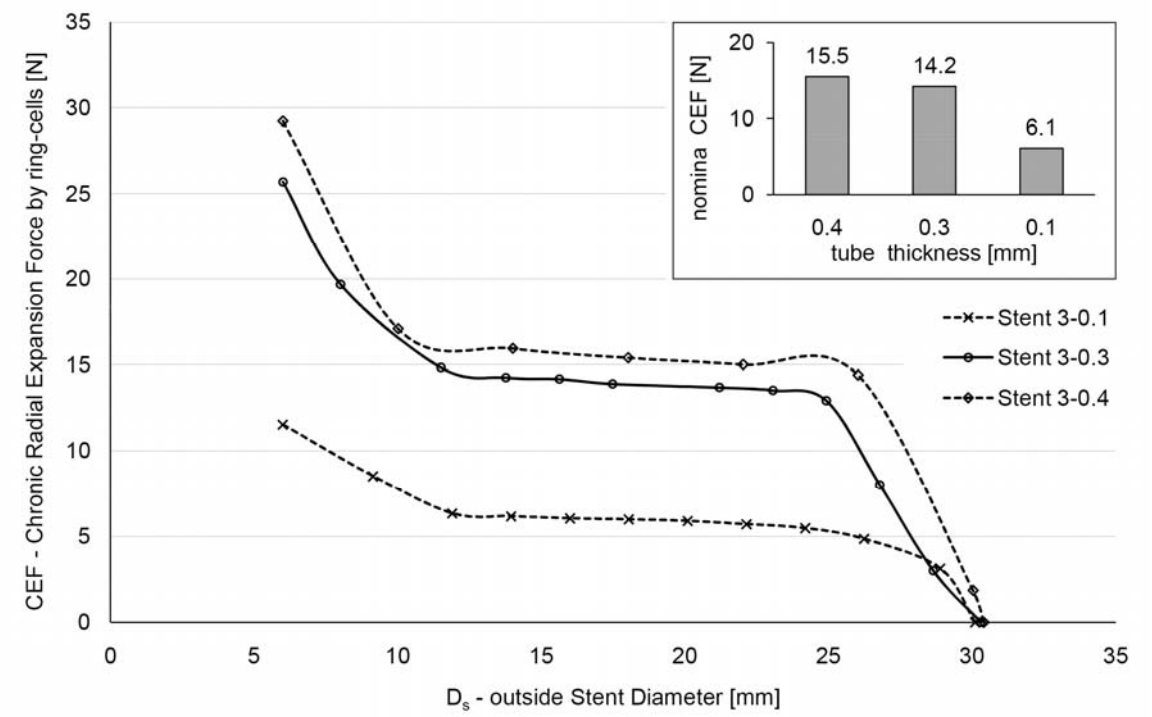

Fig. 12. Chronic Radial Expansion Force (CEF) curve for different *tube thickness*. The minimum diameter corresponds to the crimping size for a catheter of 18Fr.

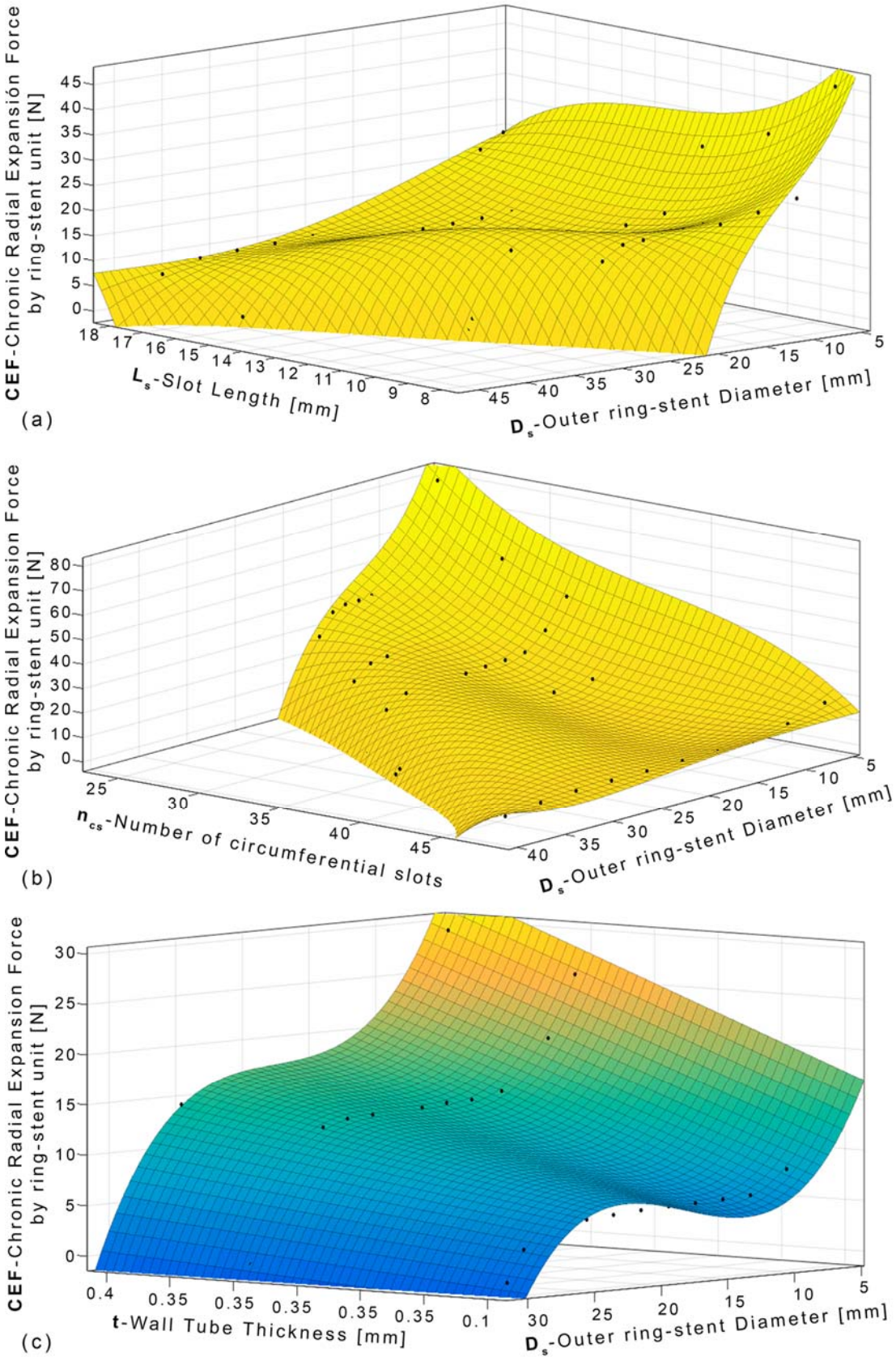

Fig. 13. Chronic Radial Expansion Force (CEF) exerted by a ring of lattice cells in function of: (a) slot length, l_s; (b) number of circumferential slots, n_{cs} and (c) tube thickness, t, for a given outer diameter in function of duct to be treated.

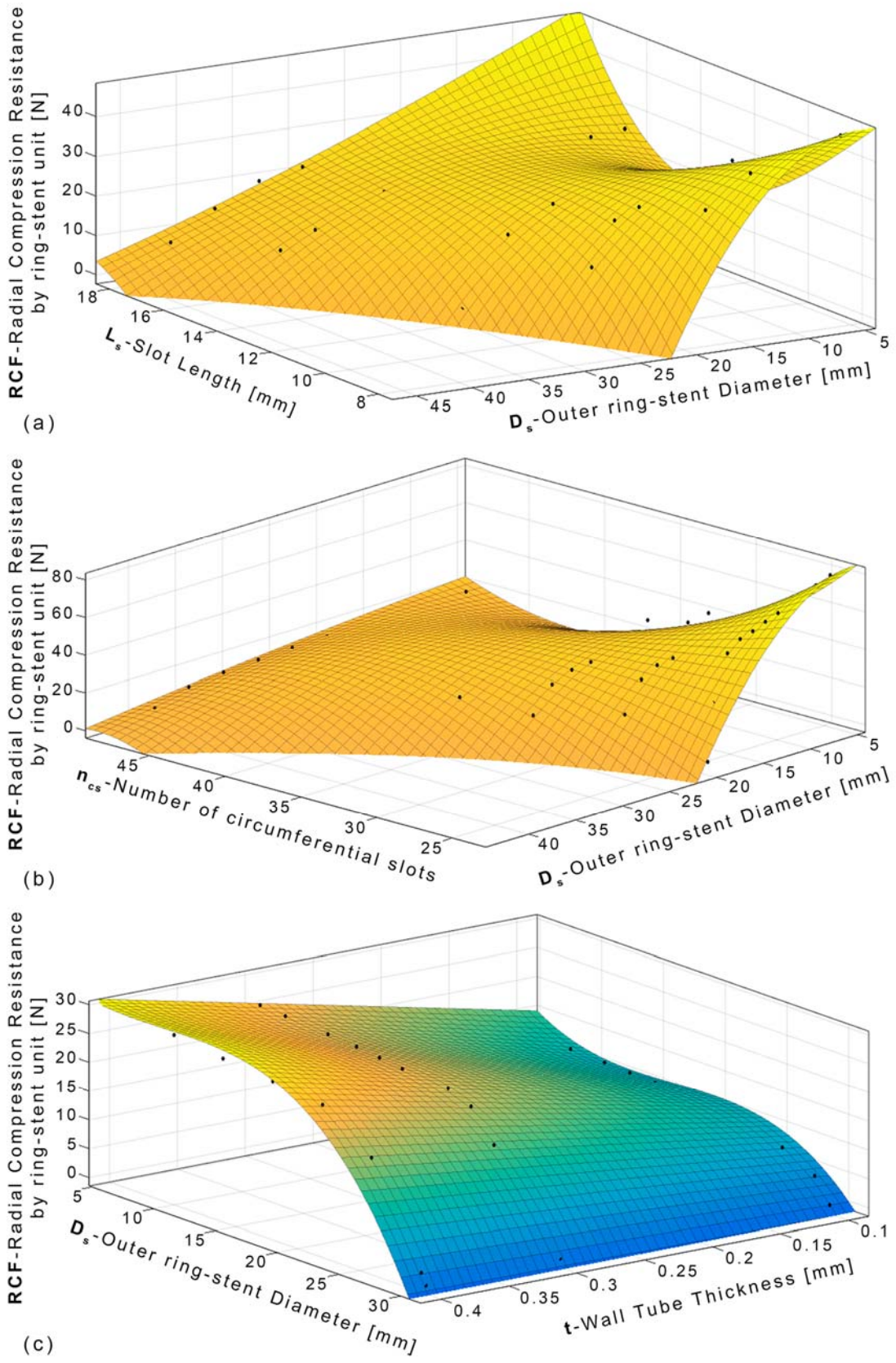

Fig. 14. Radial Compression Resistance (RCR) exerted by a ring of lattice cells in function of: (a) slot length, l_s; (b) number of circumferential slots, n_{cs} and (c) tube thickness, t, for a given outer diameter in function of duct to be treated.

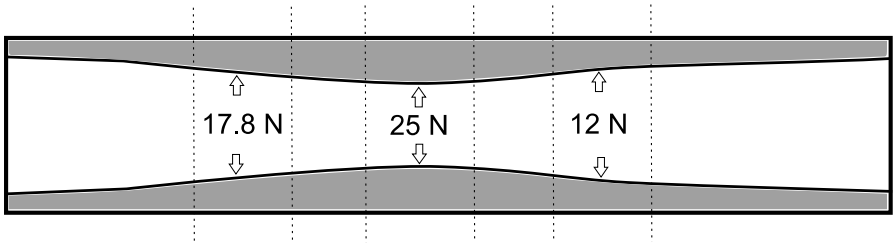

Fig. 15. Scheme of clinical specifications for a specific ill duct.

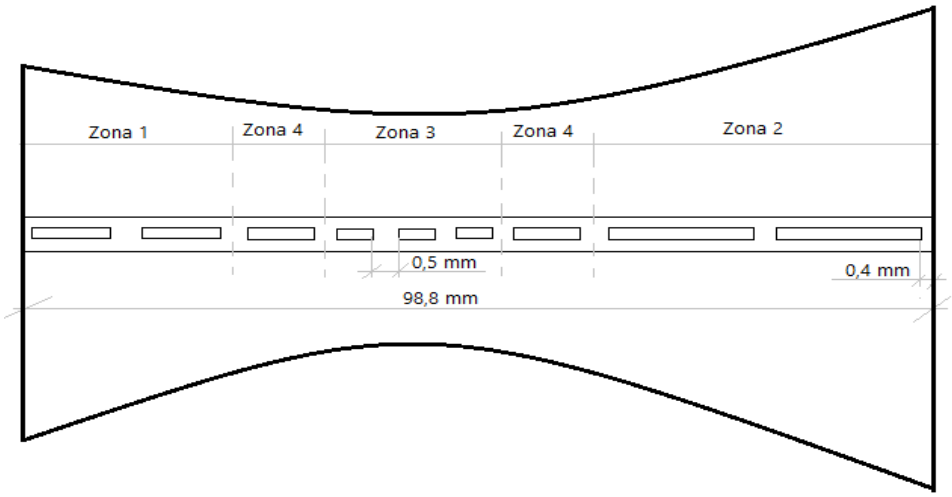

(a)

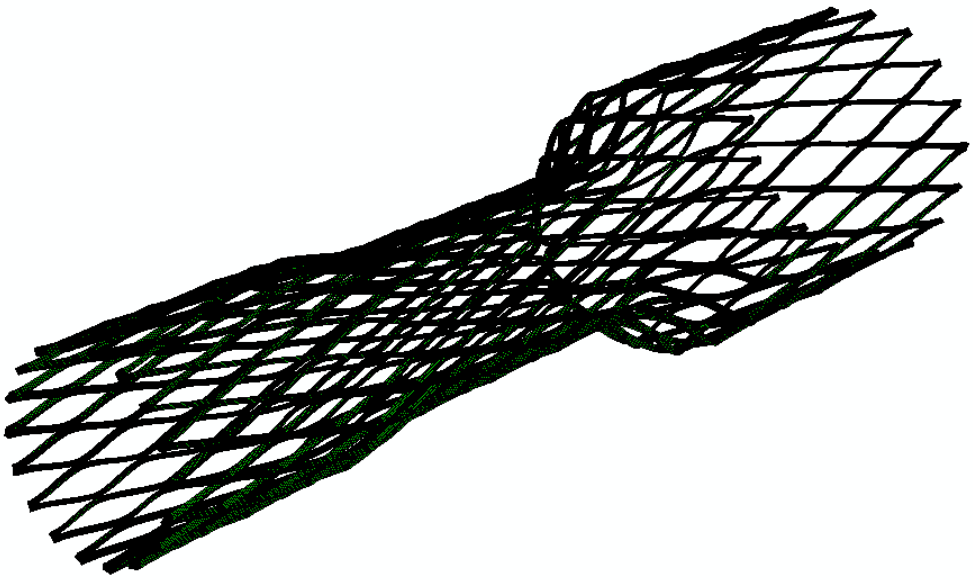

(b)

Fig. 16. (a) Scheme of cutting pattern and (b) profile adopted imposing a constant *shape factor* in every lattice-cells ring which constitutes the whole stent.